Extinction vortices are driven more by a shortage of beneficial mutations than by deleterious mutation accumulation

Walid Mawass[1,2], Joseph Matheson[1,3], Ulises Hernández[1], Jeremy J. Berg[2], Joanna Masel[1]

[1]Department of Ecology and Evolutionary Biology, University of Arizona, Tucson, AZ, 85721, USA
[2]Department of Human Genetics, University of Chicago, Chicago, IL, 60637, USA
[3]Department of Ecology, Behavior, and Evolution, University of California San Diego, San Diego, CA, 92093, USA

Corresponding author: Joanna Masel; masel@arizona.edu

Abstract

Habitat loss contributes to extinction risk in multiple ways. Genetically, small populations can face an "extinction vortex" — a positive feedback loop between declining fitness and declining population size. Two distinct genetic mechanisms can drive a long-term extinction vortex: i) ineffective selection in small populations allows deleterious mutations to fix, driving "mutational meltdown", and ii) smaller populations generate fewer beneficial mutations essential for long-term adaptation, a mechanism we term "mutational drought". To determine their relative importance, we ask whether, for a population near its critical size for persistence, changes in population size have a larger effect on the beneficial vs. deleterious component of fitness flux. In stable environments, we find that mutational drought is nearly as significant as mutational meltdown. Drought is more important than meltdown when populations must also adapt to a changing environment, unless the beneficial mutation rate is extremely high. Using simulations to capture the complex linkage disequilibria that emerge under realistically high deleterious mutation rates, we find that decreased effective population size is driven primarily by linkage disequilibria between deleterious and beneficial mutations, rather than among deleterious or among beneficials. These disequilibria modestly increase the importance of mutational drought.

Keywords: population persistence, extinction spiral, background selection, genetic hitchhiking, population genetics, census population size, evolutionary rescue

Introduction

To what degree the genetics of a population might contribute to population decline and eventual demise, and how, remains an open question [1–7]. An "extinction vortex" describes self-reinforcing feedback loops between population size and fitness, including those driven by genetic processes [8]. On short timescales, a population size reduction will increase inbreeding load via deleterious recessive alleles, lowering fitness and potentially reducing population size further [9,10]. On slightly longer timescales, the loss of standing genetic variation can undermine adaptive potential. Here, we focus on two even longer-term extinction vortices, operating over the timescale of fixation events (figure 1). First, ineffective selection in the face of stronger random genetic drift in small populations might allow a series of deleterious mutations to become fixed, in a process of "mutational meltdown". Second, fewer individuals entail fewer opportunities for the appearance of the novel mutations required for long-term adaptation, a process we call "mutational drought".

Mutational meltdown has received the most theoretical attention of the two [11–19]. Mutational meltdown is a positive feedback loop between population size N and mean fitness $\bar{W}$ (Figure 1). As a population declines in size, deleterious mutations fix more easily due to random genetic drift (Figure 1, red arrow). This decreases mean fitness $\bar{W}$, causing the population size to decline further (Figure 1, upward arrow).

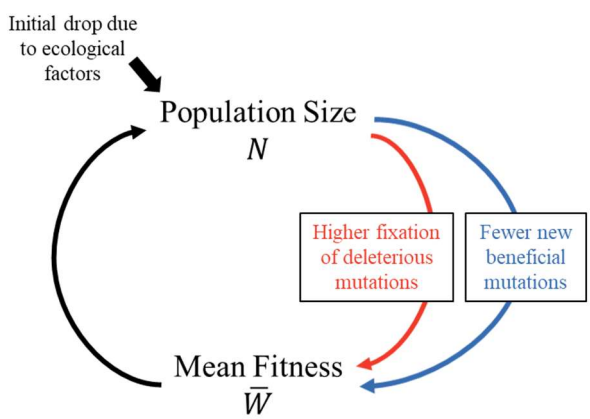

Figure 1. **An extinction vortex can be driven by the dynamics of either deleterious (mutational meltdown; red) or beneficial (mutational drought; blue) mutations**. When the net effects of deleterious fixations, environmental change, and beneficial fixations cause mean population fitness to decline, the population size N will fall. This fall in N can further exacerbate the tendency for fitness to fall, creating a positive feedback loop (extinction vortex).

Without beneficial mutations, even large populations melt down eventually. This is because some deleterious mutations are too small to be reliably purged by selection, even in large sexual populations; this has been called "Ohta's ratchet" [20]. Assuming a finite number of sites to be degraded and reversed does not solve this, but instead implies that large vertebrate species should be "dead one hundred times over" [21], unless which allele is deleterious is assumed to be conditional [22].

A solution is to include larger-effect beneficial mutations, not just reversals [23,24] . This enables compensatory asymmetry, where the fitness effects of many small effect deleterious fixations is offset by a smaller number of larger effect beneficial fixations [24–26]. The resulting long-term deleterious and beneficial "fitness fluxes" v_d and v_b are given by $UN\int p(s)p_{fix}(s)s\,ds$, where U_d or U_b gives the genome-wide rate of new mutations in each of the N individuals, producing selection coefficient s_d or s_b according to the beneficial or deleterious probability density function $p(s)$, which goes on to fix with probability $p_{fix}(s)$, changing population fitness by s.

Schultz and Lynch [23] emphasized the critical ratio of mutation rates U_b/U_d that is needed to balance deleterious and beneficial fluxes, as a function of population size N and degree of outcrossing. Here we follow Whitlock [24], who studied an essentially identical model, but instead emphasized a critical population size N_{crit} as a function of U_b/U_d. Below N_{crit}, a population crosses the threshold into an extinction vortex.

New beneficial mutations create a second, distinct positive feedback loop (Figure 1, blue arrow). Declining N reduces the number of new beneficial mutations, NU_b. (See [27] for empirical support that the beneficial mutation rate can be limiting.) This slows the adaptive increase in $\overline{W}$, which feeds back into lower N (Figure 1, upward arrow). The importance of this second feedback loop was previously briefly noted in the Discussion of [28] as an incidental finding, within a study focused on the effect of fitness function shape on extinction vortices in the context of a rapidly changing environment. We refer to this novel type of extinction vortex as "mutational drought." Adaptive fixations could be in short supply not only to counter environmental change, but also just to offset deleterious fixations under high U_d, even in the absence of environmental change.

Here we ask how much beneficial flux declines vs. deleterious flux increases as habitat loss drives a population's size down toward N_{crit}. Mathematically, how the flux changes with N near N_{crit} is captured by their derivatives with respect to population size, $\frac{dv}{dN}$, evaluated at N_{crit}. We denote this the "drought : meltdown ratio" $\left|\frac{dv_b}{dN}/\frac{dv_d}{dN}\right|_{N_{crit}}$. A ratio < 1 indicates that mutational meltdown is more important, while a ratio > 1 indicates that mutational drought is more important.

These previous models [23,24] of fitness flux $UN\int p(s)p_{fix}(s)s\,ds$ assume that each mutation evolves independently. (Complete asexuality was modelled by [29], but is less relevant for most endangered populations.) However, the independence assumption is violated by background selection caused by deleterious mutations, and by hitchhiking and clonal interference caused by beneficial mutations [30,31]. These phenomena increase the fixation probabilities of deleterious mutations and decrease those of beneficial mutations.

In the process, in a finite population, both deleterious [32] and beneficial [33] mutations cause linkage disequilibrium (LD), accounting for the non-independence. Importantly, LD has been shown to accelerate mutational meltdown [14]. LD has been detected even among unlinked sites [34,35]. It will arise when $U_d > 1$, from background selection among unlinked sites, which is more powerful than background selection among linked sites in this regime [36].

The evidence for $U_d > 1$ is clearest for humans. A lower bound was derived [37] by assuming that mutations are deleterious only in the 55% of the 6×10^9 base pairs in a diploid genome that are not dominated by dead transposable elements shared with chimpanzees, and that this 55% of the genome evolves 5.7% slower due to this constraint [38], implying that 5.7% of mutations were deleterious enough to be purged by natural selection. A conservative point mutation rate of 1.16×10^{-8} per base pair per replication [39] then yields $U_d > 0.55\times6\times10^9\times0.057\times1.16\times10^{-8} = 2.2$ per replication. This estimate is conservatively low, for five reasons. First, some mutations to transposable element regions are deleterious. Second, 1.16×10^{-8} is the lower bound of a 95% confidence interval on the point mutation rate [39]. Third, non-point mutations and beneficial mutations are neglected. Fourth, the constraint estimate [38] came from reference genomes that include some derived polymorphisms, which are less constrained than fixed differences. Fifth, under a distribution of fitness effects (DFE), some weakly deleterious mutations fix, and will not be included within the 5.7%. Some therefore argue that the human deleterious mutation rate is as high as $U_d = 10$ [40,41]. Humans have only a modestly higher point mutation rate than most other eukaryotes [39], making it likely that $U_d > 1$ is common.

Capturing unlinked LD arising from $U_d > 1$ requires simulating the entire genome rather than just a genomic region. This is computationally infeasible for most forward-time simulators (e.g., SLiM, [42], because the number of segregating mutations to be tracked scales with $U_d N$, which becomes too large. Here we conduct whole genome simulations using a recently developed approach [26] that assumes that recombination occurs only at hotspots; we track only a summary of each "linkage block" (between hotspots), avoiding the need to track every segregating mutation.

Here we ask how important mutational drought is relative to mutational meltdown, as a function of three main factors: 1) U_d/U_b, 2) the rate of environmental change, if any, and 3) the presence or absence of LD. We also ask how LD lowers both N_{crit} and N_e (i.e. expected coalescence time of a neutral allele) in the corresponding regime. Specifically, we investigate the extent to which reduced N_{crit} and N_e are driven by background selection (deleterious alleles decreasing neutral diversity, decreasing beneficial flux and increasing deleterious flux), hitchhiking (beneficial alleles decreasing neutral diversity and increasing deleterious flux), and/or clonal interference among beneficials (decreasing beneficial flux).

Methods

1. Without linkage disequilibrium (LD)

Fixation probability. Independent evolution of each site (i.e. no LD nor epistasis) enables an analytical, one locus approach. Each copy of a mutation affects fitness by a factor of $(1+s)$. To facilitate comparisons with simulations, we capture co-dominance not via a dominance coefficient $h = 0.5$, but by reducing fitness by $(1+s)^2$ for homozygous mutants. The exact probability of fixation $p_{fix}(s)$ of a new mutation under the Moran birth-death process is then $p_{fix}(s) = \frac{1-e^{-2s}}{1-e^{-4Ns}}$. We take this from Equation 1 of [43], adjusted for a diploid population of size N. It is exact for Malthusian fitness; per-generation fitness yields the same when an approximation is used [44].

Deleterious fitness flux. The best-studied distribution of $2N_e s_d$ was inferred from the human site frequency spectrum of non-synonymous mutations [45] as a gamma distribution $p_d(-2N_e s_d) = \frac{e^{\frac{-2N_e s_d}{\beta}} \, 2N_e s_d{}^{-1+\alpha} \beta^{-\alpha}}{\Gamma(\alpha)}$, where $\Gamma(\alpha)$ is the gamma function, $\alpha = 0.169$ is the shape parameter, and $\beta = 1327.4$ is the scale parameter. We divide by $2N_e$ = 23,646 (from their Table 2, row 9), yielding a DFE for non-synonymous s_d with α = 0.169, β = 0.056.

Many deleterious mutations occur in non-coding regulatory regions such as enhancers and promoters [46], and may have smaller mean deleterious effect size ($\bar{s}_d$) [47]. Structural mutations might have larger $\bar{s}_d$. We therefore varied $\bar{s}_d$ by varying the scale parameter while keeping the shape parameter fixed.

The deleterious fitness flux, i.e. the rate population fitness declines due to deleterious fixations, is equal to the per-generation rate of new mutations $U_d N$, times their fixation probability $p_{fix}(s_d)$, times their homozygous impact on fitness $2s_d$ once fixed: $v_d = U_d N \int_{-\infty}^{0} p_d(s_d)\, 2s_d\, p_{fix}(s_d)\, ds_d$.

Beneficial fitness flux. We follow others (e.g. [24]) to assume an exponential DFE with mean $\bar{s}_b$, $p_b(s_b) = \frac{1}{\bar{s}_b}\, e^{-s_b/\bar{s}_b}$. The beneficial fitness flux is $v_b = U_b N \int_0^{+\infty} p_b(s_b) 2s_b\, p_{fix}(s_b)\, ds_b$.

Critical population size. We calculated the deleterious and beneficial fitness fluxes numerically in Mathematica 14.2.3 (Supplementary Notebook), using the DFEs above. The environmental change rate δ_{env} is either zero or in the range δ_{env}= -10^{-6} to -$10^{-3.5}$. We express the environmental change rate, for ease in interpretation, as the number of generations over which environmental change reduces fitness

by 10%, with $-0.1/\delta_{env} = 10^5$ to $10^{2.5}$ generations. We consider even the fastest of these environmental change rates low because deleterious fixations cause more fitness loss than environmental change does. Coevolution, especially with parasites, likely makes the biggest contribution to δ_{env} [48].

We solve for N_{crit} as the value of N for which $v_{net} = v_b + v_d + \delta_{env} = 0$, and calculate the drought : meltdown ratio as $\left|\frac{dv_b}{dN}\Big/\frac{dv_d}{dN}\right|_{N_{crit}}$. With linkage equilibrium, $N_e = N$.

The beneficial mutation rate and effect sizes will be larger in worse-adapted populations, which is hard to capture within the standard relative fitness formulation of population genetics. Higher U_d and δ_{env} would make populations worse adapted if all else were held equal but are offset by higher N_{crit}. Future work on less conventional models of absolute fitness under density-regulation (e.g., [49,50]) would be needed to explore the exact balance between these two factors. Until then, the fact that there is a balance helps justify our use of constant U_b and $\bar{s}_b$.

2. With LD

Simulation setup. Our forward time simulation method is described in [26]. Briefly, each genome consists of two haplotypes, divided into 23 chromosomes, further segmented into non-recombining 'linkage blocks'. The fitness impacts of all mutations i within a given allele of linkage block j are summarized as $l_j = \prod_i (1 + s_i)$. Individual fitness combines L linkage blocks across two haplotypes as $w = \prod_{j=1}^{L}(l_{j,1}) \prod_{j=1}^{L}(l_{j,2})$. We employ a Moran model with a constant population size N, where individuals are chosen to reproduce based on their fitness.

Recombination occurs only at hotspots between adjacent linkage blocks. We simulated two recombination events per chromosome per meiosis [51]. We used 100 linkage blocks per chromosome for computational efficiency, which previous work found to be more than sufficient [26].

We sampled the numbers of new deleterious and beneficial mutations from Poisson distributions with means U_d and U_b, respectively. We sampled selection coefficients from the DFEs above.

Simulations ran for $100N$ generations. Following [26], we ended a burn-in phase away from a clonal initial population 100 generations after a linear regression of the variance in fitness over the last 200 generations produced a slope less than $0.07/N$. Net fitness flux v_{net} was estimated post burn-in as the slope $\hat{v}_{net}$ of log mean population fitness over time, without decomposition into v_d and v_b.

Critical population size. N_{crit} is defined as the value of N for which $v_{net} = 0$, but $\hat{v}_{net}$ estimation is too noisy to find N_{crit} using purely deterministic root-finding methods, especially for small values of N_{crit}. We first bracketed N_{crit}, with N = 1500 and 6000 as initial guesses, progressing outward by a factor of two as needed until we had $\hat{v}_{net}$ values both above and below zero. Then we iterated the secant method until $\hat{v}_{net}$ changed by < 15%. Then we fitted a straight line to all evaluated $\{N, \hat{v}_{net}\}$ data points for which N was within a factor of 3 from the final evaluated value. We estimated N_{crit} as the zero for this fitted line.

<u>*Drought : meltdown ratio*</u>. We estimated v_d and v_b from the set of mutations whose time of final fixation lay between the end of the burn-in phase and the end of the run. Tracking fixations does not exactly track mean population fitness due to fluctuations caused by polymorphisms. For computational efficiency, the simulations described so far summarize the fitness of many mutations per linkage block, making information about individual fixed mutations inaccessible. In simulations intended to estimate the drought : meltdown ratio, we made them accessible via tree sequencing recording [52] tracking all non-neutral mutations, including their time of fixation. We calculated $v_d = \frac{\sum_{i=1}^{n_d} 2s_{d,i}}{G^*}$ and $v_b = \frac{\sum_{i=1}^{n_b} 2s_{b,i}}{G^*}$,

where G^* is generations elapsed since burn-in ended, and n_d and n_b are the numbers of deleterious and beneficial mutations that fixed during this time.

We numerically estimated $\frac{dv_b}{dN}$ and $\frac{dv_d}{dN}$ as $\frac{dv}{dN} = \frac{v(N_{crit}+\varepsilon) - v(N_{crit}-\varepsilon)}{2\varepsilon}$, where we chose $\varepsilon = 150$ individuals as a balance between reducing noise and avoiding curvature in v. We do this by running simulations for $N_{crit} + \varepsilon$ and $N_{crit} - \varepsilon$.

Results

Without LD, where $N_e = N$, Whitlock's [24] choice of $U_d/U_b = 1000$, combined with the deleterious DFE from [45], and a conservatively low $\bar{s}_b = 0.001$, yields $N_{crit} \simeq 1834$ (Figure 2A, solid blue and red lines intersecting at dotted red vertical line). Equation (9) from [24] produces a substantial underestimate: $N_{crit} \cong \sqrt[3]{\frac{U_d}{64\,\bar{s}_b{}^2|\bar{s}_d|U_b}} = 1181$, after assuming an exponential deleterious DFE to simplify [24]'s Equation 3 expression for v_d. However, the coefficient of variation is ~2.4, far from 1, in the empirically inferred deleterious DFE of [45]. If we instead use [24]'s Equation (3), we obtain a less inaccurate $N_{crit} \simeq 1967$. Figure S1 illustrates similar agreement across the range of U_d/U_b values. We note that N_{crit} values in [24] are intended to represent N_e not census N.

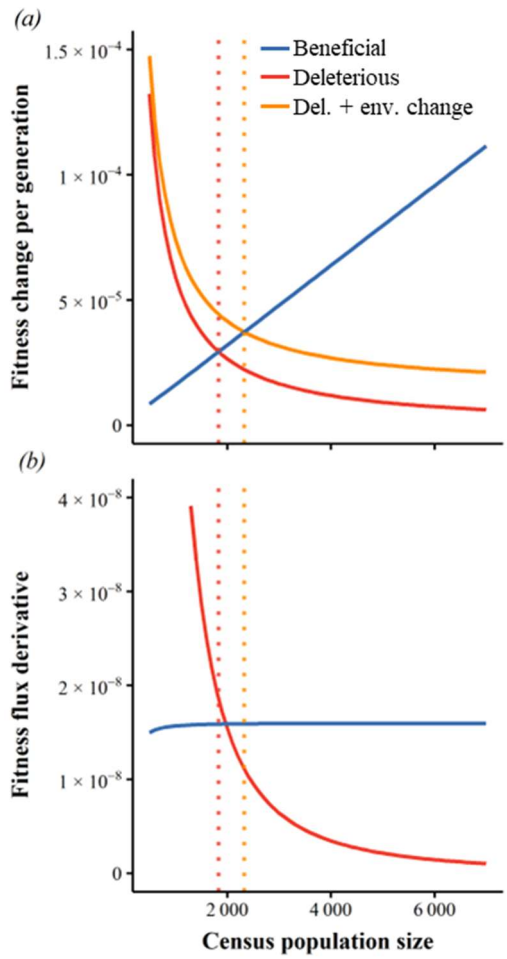

Figure 2. **Extinction vortices are driven more by mutational drought than by mutational meltdown.** Vertical lines indicate N_{crit}, defined by the intersection in (a) of beneficial fitness flux (blue) with either deleterious fitness flux (red), or with deleterious flux plus environmental deterioration (orange). Environmental change adds a constant δ_{env} = -1.5×10^{-5} per generation to deleterious flux in (a) and hence does not change its slope (red line in (b)). The ratio of the y-values in (b) at N_{crit} indicates the relative

importance of mutational drought (blue) vs. mutational meltdown (red). U_d = 2, $U_d/U_b = 1000$, $\bar{s}_b$ = 0.001, $\bar{s}_d$ = -0.009 via the DFE from [45], and there is linkage equilibrium.

At N_{crit} in the absence of environmental change (dotted red vertical line in figure 2B), declining N has 85% of the impact on beneficial flux as it has on the deleterious flux that is normally assumed to be the sole cause of an extinction vortex according to mutational meltdown theory. When adaptation must also counter environmental change, larger populations enter the extinction vortex (figure 2a, orange vertical dotted line illustrates $N_{crit} \simeq 2330$ when environmental change reduces fitness by 10% over ~6,000 generations). Even modest environmental change makes the impact of declining N on beneficial flux larger than that on deleterious flux (blue line is above red along dashed orange vertical line in figure 2b). In other words, environmental change makes mutational drought more important than mutational meltdown.

Indeed, the drought : meltdown ratio is > 1 with $U_d/U_b = 1000$ when slow environmental change causes fitness to decline by 10% over as many as ~20,000 generations (figure 3a, right, grey, dot-dashed vertical line). When U_b is 10 times higher, faster but still modest environmental change is needed to drive the drought : meltdown ratio > 1 (figure 3a, left, blue, dot-dashed vertical line, ~4000 generations for fitness to decline by 10%). We interpret both these rates of environmental decline as rather slow because they correspond to only 0.19× and 0.28× the rates of fitness decline due to deleterious fixations for U_d = 2 (figure 3b, colour-matched intersections with vertical lines). Environmental change can drive the drought : meltdown ratio > 1 without excessively elevating N_{crit} (figure 3c steep rise in N_{crit} occurs well to the left of the color-matched vertical line).

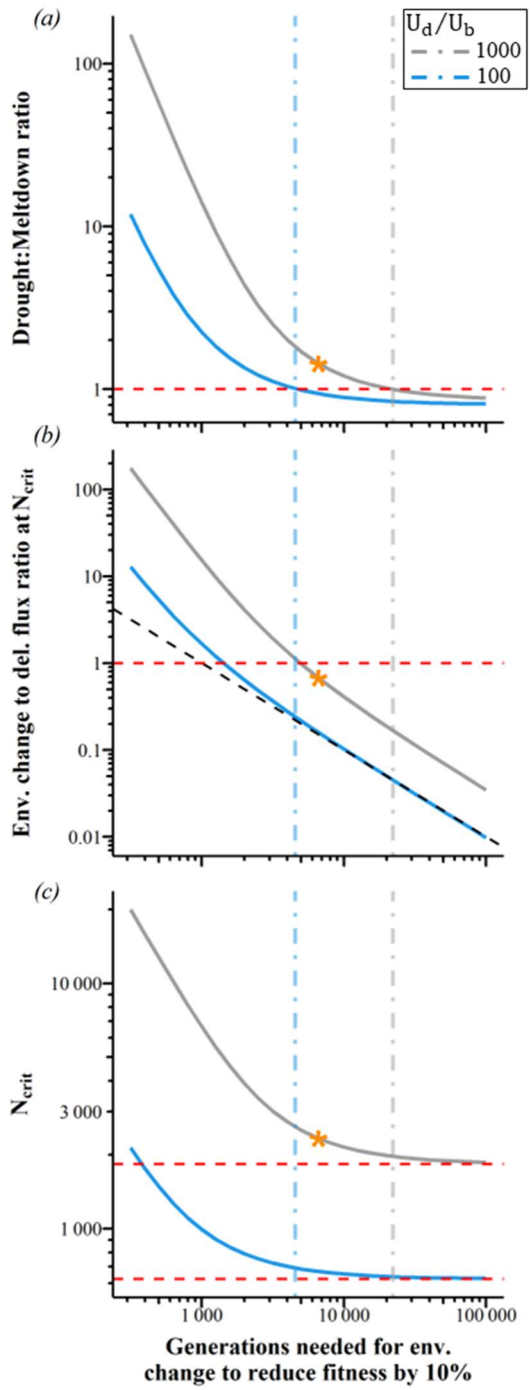

Figure 3. **Slow environmental degradation is sufficient to make mutational drought more important than mutational meltdown.** $\bar{s}_b$ = 0.001, U_d = 2, $\bar{s}_d$ = -0.009 via the DFE from [45]. Linkage equilibrium is assumed. The orange star indicates the example shown in figure 2. Vertical lines represent where the drought : meltdown ratio = 1. (b) We consider environmental change to be relatively slow below the red dashed horizontal line, where mutational degradation makes a bigger contribution to fitness decline. Diagonal black dashed line in (b) represents proportionate change in the x-axis and y-axis; departure from this indicates increased deleterious flux in the face of rapid adaptation. Red dashed lines in (c) indicate asymptotes, i.e. no environmental change.

When beneficial mutations are scarce (higher U_d/U_b), mutational drought is relatively more important, with the drought : meltdown ratio saturated by the U_d/U_b~1000 value (figure 4a) used in

figure 2. Lowering U_b has two opposing effects. First, it proportionately lowers the beneficial fitness flux v_b and its derivative $\frac{dv_b}{dN}$ (i.e. it reduces the slope of the blue line in figures 2A and consequently reduces the height of the blue line in figure 2B). Second, lower v_b moves the intersection N_{crit} to the right, i.e. towards larger values of N, which lowers $\left.\frac{dv_d}{dN}\right|_{N_{crit}}$ without substantially changing $\left.\frac{dv_b}{dN}\right|_{N_{crit}}$ (figure 2B, red and blue lines, respectively). The flat drought : meltdown ratio to the right of figure 4a shows that when beneficial mutations are scarce at high $U_d/U_b \geq 1000$, these two effects cancel each other out.

Weaker beneficial effects (figure 4b), and stronger deleterious effects (figure 4c) make mutational drought only slightly less important. These effects are only slightly larger when beneficial mutations are more common (figures 4b and 4c dashed curves). This makes our results insensitive to the difficulties of empirically inferring selective effect sizes.

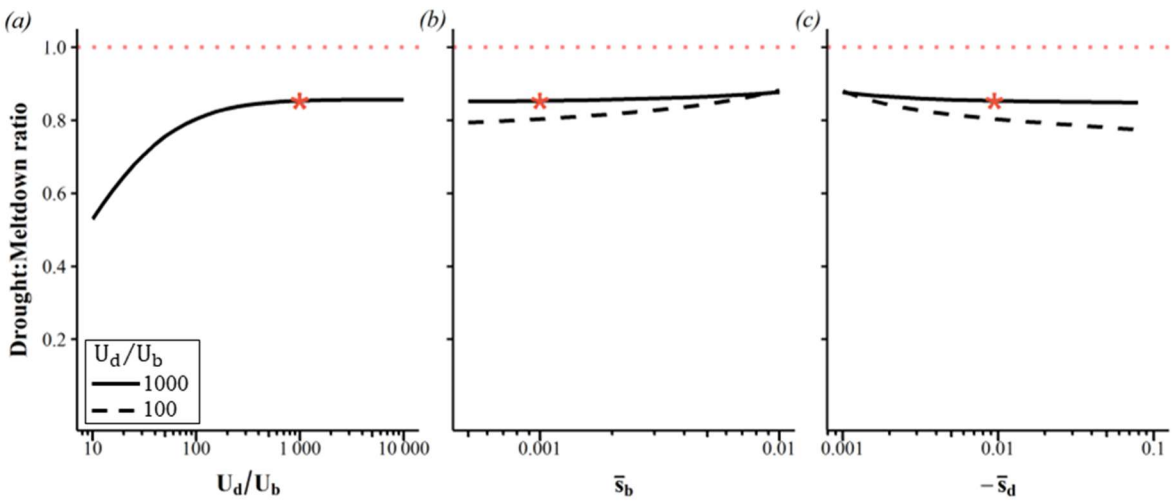

Figure 4. **The drought : meltdown ratio is fairly insensitive to parameter value choices.** Linkage equilibrium is assumed, with no environmental change. (a) Mutational drought becomes somewhat less important when (a) beneficial mutations are abundant, (b) beneficial effects are weak, and (c) deleterious effects are strong. Where not otherwise specified, $\bar{s}_d$ = 0.009 via the DFE from [45], $\bar{s}_b$ = 0.001. U_d = 2 throughout, but results for different U_d are superimposable. The red star indicates the example shown in figure 2 with no environmental change. See figure S2 for corresponding changes in N_{crit}.

With environmental change, dependence on U_d and U_b does not simplify to dependence on their ratio, as in figure 4a. We illustrate this in figure 5 for two environmental change scenarios: for the dashed lines, environmental change is swamped by deleterious mutation accumulation, whereas for the solid lines, environmental change is more substantial albeit never exceeding mutational degradation (figures 5b and 5e). When faster environmental change and more scarce beneficial mutations push the drought : meltdown ratio above 1 (figures 5a and 5b), lower U_d makes mutational drought more rather than less important (figure 5a). The drought : meltdown ratio only falls substantially below 1 under the slower environmental change scenario, and only when U_d/U_b is small (figure 5a, left portion of dashed blue). This corresponds to exceptionally small N_{crit} (figure 5c). Under realistically high U_d, high drought : meltdown ratios are found when beneficial mutations are scarce (figure 5d, solid lines to right), making N_{crit} high (figure 5f), and thus environmental change at N_{crit} is relatively fast compared to a slower rate of deleterious fixations (figure 5e). The drought : meltdown ratio is mostly insensitive to selection coefficients, although it rises for very small $\bar{s}_b$ (figure S3).

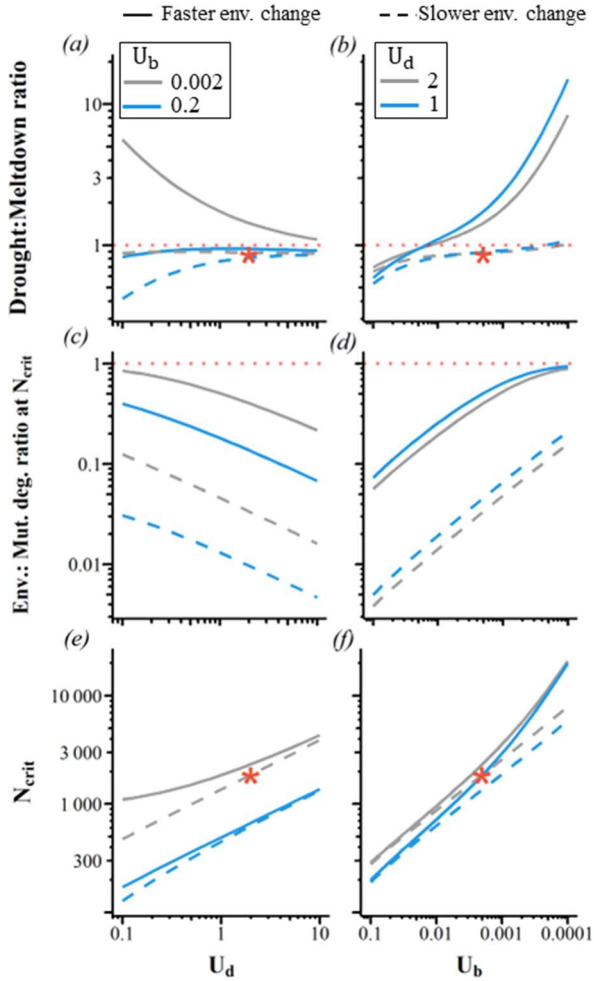

Figure 5. The drought : meltdown ratio only falls substantially below 1 for very low N_{crit}. (a) Faster environmental degradation, combined with low U_b, can make mutational drought more rather than less important for lower U_d. (a) and (d) can be compared to the constant environmental case in figure 4a, where only the ratio U_d/U_b matters. Reverse scaling of the U_b x-axis of (d), (e) and (f) is used to facilitate comparison of (d) with (a) and with figure 4a. Solid lines represent a fitness reduction of δ_{env}= -1.5×10^{-5} per generation, matching the example in figure 2, and dashed lines represent δ_{env} = -10^{-6}; impact relative to deleterious flux is contextualized in (b) and (e). Our slower environment is comparable to the constant environment example from figure 2 (red star). Independent sites model with $\bar{s}_b$ = 0.001 and $\bar{s}_d$ = -0.009 via the DFE from [45].

The presence of LD, which we capture in simulations with U_d = 2 and no environmental change, produces a modest 8% increase in the drought : meltdown ratio, from 0.85 to 0.92, as beneficial flux becomes slightly more sensitive to N (figure 6d, blue points are above blue line). This goes away when we quantitatively reduce LD by increasing the number of chromosomes from 23 to 50 (figure S4a).

LD increasing N_{crit} from 1834 to 4403 (figure 6a, solid dots), in a way that is qualitatively robust to adding more chromosomes (figure S4b). The $N = 4403$ population with LD can thus been seen to have $N_e = 1834$, such that $\frac{N_e}{N} = \frac{1834}{4403}$. Beyond N_{crit}, rescaling describes v_d and v_b well, as seen by the close match between analytical lines and simulated points when the x-axes of figures 6a and 6c are rescaled according to $N_e = N\frac{\text{analytical } N_{crit}}{\text{simulated } N_{crit}}$ to produce figures 6b and 6d. LD slightly increases the magnitude of fitness fluxes at their $v_d = v_b$ intersection (figure 6b).

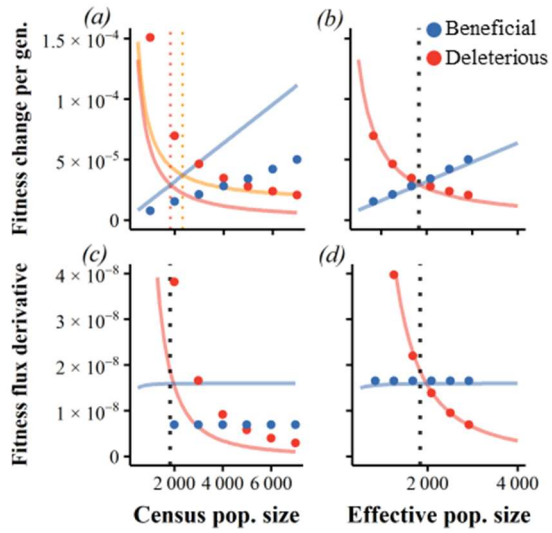

Figure 6. Linkage disequilibrium makes mutational drought slightly more important. Continuous red and blue lines are analytical results given linkage equilibrium, while dots are simulation results with LD. (a) and (b) add simulation results to the static environment example of figure 2. In (c) and (d), the x-axis for simulation results is scaled such that intersection occurs at the same "effective" N_{crit} as found without LD. U_d = 2, $U_d/U_b = 1000$, $\bar{s}_b$ = 0.001, $\bar{s}_d$ = -0.009 via the DFE from [45].

The reduction in N_e could be due to beneficial mutations interfering with each other (clonal interference decreasing beneficial flux), and/or hitchhiking (beneficial mutations increasing deleterious flux), and/or background selection (deleterious mutations both decreasing beneficial flux and increasing deleterious flux). In figure 6, background selection from deleterious mutations on deleterious or neutral mutations (using eq. (4) in Matheson and Masel 2024) predicts a ratio of $N_e/N = 0.82$, but we see a ratio of $\frac{\text{analytical } N_{crit}}{\text{simulated } N_{crit}}$ = 0.42. A model of deleterious mutations alone thus accounts for only (1 – 0.82)/(1 – 0.42) = 30% of the reduction in effective N_{crit}. When we measure N_e the usual way, as the expected coalescent time, the factor reduction in N_e (figure 7, blue triangles) matches the reduction in fitness fluxes and hence N_{crit} (figure 7, black circles), but not that predicted by deleterious mutations alone (figure 7, red squares).

If low N_e were due to clonal interference, then the reduction in N_e should be stronger for high U_b and s_b, but the (very weak) trends are in the opposite direction (figures 7a and 7c). Since neither beneficial mutations alone (clonal interference) nor deleterious mutations alone can explain our results, this points to an interaction between deleterious and beneficial mutations. There are two kinds of interaction: beneficial mutations increase the fixation probability of deleterious mutations [53,54], and deleterious mutations decrease the fixation probability of beneficial mutations [55,56]. From the fact that deleterious and beneficial fluxes scale in the same way in figure 6, we deduce that both happen to the same degree. This interpretation explains greater N_e reduction for large U_d and s_d (figures 7b and 7d); variance in fitness due to deleterious alleles scales with $U_d s_d$ [37,57]. Larger U_b and s_b could make deleterious mutations less important, explaining the lesser reduction in N_e (figures 7a and 7c).

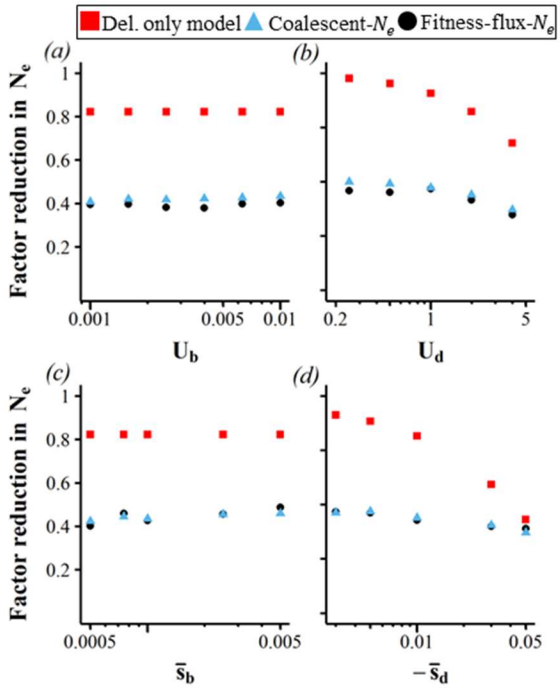

Figure 7. **The degree to which effective population size is reduced below census size suggests the interplay between deleterious and beneficial mutations.** $\frac{\text{analytical } N_{crit}}{\text{simulated } N_{crit}}$ (black dots) is close to N_e/N from coalescence time (blue triangles). Where not otherwise specified, $\bar{s}_b$ = 0.001, U_d = 2, U_b = 0.02, and $\bar{s}_d$ = -0.009 via the DFE from [45]. Model of deleterious mutations alone is from Equation 4 in [36]. There is no environmental change.

Discussion

Mutational meltdown describes an extinction vortex in which small populations cannot purge slightly deleterious mutations, whose fixations handicap the population, making it still smaller. Here, we find that a shortage of beneficial mutations appearing in smaller populations creates mutational drought, a distinct kind of extinction vortex. Mutational drought is only slightly less significant than mutational meltdown in the absence of environmental change and becomes more important in the more realistic scenario of even a slowly changing environment. Mutational drought is modestly more significant with LD, and more significant when beneficial mutations are rare. Beneficial mutations are thus either common, or else their population-size-dependent scarcity is critical – in neither case can population genetic models ignore beneficial mutations. Near the critical census population size, the reduction in effective population size is best explained by interactions between beneficial and deleterious mutations.

The role of beneficial mutations in population persistence studied here plays out over much longer timescales than processes of "evolutionary rescue" in previous population genetic (discrete) models, although in line with the broader use of the term in the context of quantitative genetics models (see [28]). In the broad sense, evolutionary rescue refers to scenarios where genetic adaptation struggles to keep up with ongoing environmental change, over an indefinitely long period of time [58–62]. Within the narrow sense, population genetic models consider a population whose birth rate is initially less than its death rate, e.g. following a single abrupt environmental change that can be remedied by one or several beneficial mutation(s) [63–68]. Here we use a population genetic model to consider evolutionary rescue in the broad sense more commonly treated by quantitative genetic models, across an indefinitely long series of beneficial and deleterious fixations. Given ongoing environmental change, we find that

mutational drought, not mutational meltdown, is the dominant process driving the extinction vortex. Indeed, mutational drought is nearly as important, even in the total absence of environmental change.

Conservation management and species recovery programs assess the 'minimum viable population' (MVP) and the factors influencing it [69–72]. We follow [73] in defining N_{crit} as the lowest population size that avoids an extinction vortex. This is a different kind of MVP to the usually considered empirical predictor of probability of persistence after a specified period of time, e.g. 1000 years [72,74]. Our N_{crit} concerns the ability to resupply the population with new beneficial mutations to balance both the accumulation of deleterious mutations, and ongoing environmental change, to achieve long-term viability. N_{crit} is the gateway to the extinction vortex below which some combination of mutational meltdown and mutational drought contribute. Our N_{crit} is relevant over the long timescales of multiple sweeps making our results applicable more clearly to species than to populations, reliant on mutation rather than migration as the source of new variants.

The reduction from N to N_e is primarily caused by LD between beneficial and deleterious mutations. A model of background selection among linked deleterious mutations alone (excluding the larger contributions of LD among unlinked deleterious mutations [36]) is sometimes considered as the best explanatory model of genetic diversity patterns [75–77], e.g., via one-locus models that use a B factor to rescale N_e [78]. Our results here suggest that such a model will underestimate the degree to which LD reduces N_e and N_{crit} in the parameter value regime of interest to species of conservation concern.

The assessed extinction risk of vertebrate species in the Anthropocene [79] includes assessed long-term risks to environmental conditions [80]. Current conservation efforts often focus on emergency revitalization programs with tools that might only achieve short-term persistence (e.g., [81], potentially creating trade-offs between long-term and short-term objectives [82]. Short-term goals may be problematically prioritized under triage from restricted budgets [83,84] over achieving long-term sustainable populations [85,86].

Some conservation geneticists advocate genetic rescue, whereby gene flow from a few introduced individuals helps small fragmented populations [87–89]. The genetic rescue paradigm aims to maximize genetic diversity to reduce the risk of extinction [87,90,91]. However, gene flow from large, outbred populations may introduce too many recessive deleterious alleles to be easily purged, with deleterious effects that might quickly have devastating consequences within a small inbred population [6,92,93]. Abandoning the genetic rescue paradigm might limit the risk of deleterious accumulation in the short term. Our results on mutational drought help emphasize that this might still be a mistake over longer timescales if a shortage of adaptive mutations later poses an extinction risk. Fortunately, according to simulations, the benefits of genetic rescue can be obtained while minimizing harm by steadily introducing migrants from other small inbred populations from which recessive deleterious mutations are already purged [6,93], as has occurred naturally in Florida scrub-jays [94].

Acknowledgements

We thank Daniel Smith, Ryan Gutenkunst, Elise Lauterbur, and David Enard for their thoughtful comments on parts of this study, and Naman Panday for sharing his git expertise. We also thank Jerome Kelleher, Peter Ralph, and Yan Wong for helpful discussions about tree sequence recording.

Funding

This study was funded by the John Templeton Foundation (62028) and by NIH R35 grant (GM151257). The funders had no role in study design, data collection and analysis, decision to publish, or preparation of the manuscript.

Data Availability

Analytical results conducted in Wolfram Mathematica. Simulation code was written in C, and graphs produced with R. Simulation code and scripts have been archived at [95].

Conflict of interest

All authors declare no conflicts of interest.

References

1. Keller LF, Waller DM. 2002 Inbreeding effects in wild populations. *Trends Ecol. Evol.* **17**, 230–241. (doi:10.1016/S0169-5347(02)02489-8)

2. Spielman D, Brook BW, Frankham R. 2004 Most species are not driven to extinction before genetic factors impact them. *Proc. Natl. Acad. Sci.* **101**, 15261–15264. (doi:10.1073/pnas.0403809101)

3. Frankham R. 2005 Genetics and extinction. *Biol. Conserv.* **126**, 131–140. (doi:10.1016/j.biocon.2005.05.002)

4. Fox CW, Reed DH. 2011 Inbreeding Depression Increases with Environmental Stress: An Experimental Study and Meta-analysis. *Evolution* **65**, 246–258. (doi:10.1111/j.1558-5646.2010.01108.x)

5. Kardos M, Armstrong EE, Fitzpatrick SW, Hauser S, Hedrick PW, Miller JM, Tallmon DA, Funk WC. 2021 The crucial role of genome-wide genetic variation in conservation. *Proc. Natl. Acad. Sci.* **118**, e2104642118. (doi:10.1073/pnas.2104642118)

6. Kyriazis CC, Wayne RK, Lohmueller KE. 2021 Strongly deleterious mutations are a primary determinant of extinction risk due to inbreeding depression. *Evol. Lett.* **5**, 33–47. (doi:10.1002/evl3.209)

7. Dussex N, Morales HE, Grossen C, Dalén L, Oosterhout C van. 2023 Purging and accumulation of genetic load in conservation. *Trends Ecol. Evol.* **38**, 961–969. (doi:10.1016/j.tree.2023.05.008)

8. Giplin ME, Soulé ME. 1986 Minimum viable populations : Processes of species extinction. *Conserv. Biol. Sci. Scarcity Divers.* , 19–34.

9. Tanaka Y. 2000 Extinction of populations by inbreeding depression under stochastic environments. *Popul. Ecol.* **42**, 55–62. (doi:10.1007/s101440050009)

10. Fagan WF, Holmes EE. 2006 Quantifying the extinction vortex. *Ecol. Lett.* **9**, 51–60. (doi:10.1111/j.1461-0248.2005.00845.x)

11. Lynch M, Gabriel W. 1990 Mutation Load and the Survival of Small Populations. *Evolution* **44**, 1725–1737. (doi:10.1111/j.1558-5646.1990.tb05244.x)

12. Gabriel W, Lynch M, Bürger R. 1993 Muller's Ratchet and Mutational Meltdowns. *Evolution* **47**, 1744–1757. (doi:10.1111/J.1558-5646.1993.TB01266.X)

13. Lynch M, Conery J, Bürger R. 1995 Mutational Meltdowns in Sexual Populations. *Evolution* **49**, 1067–1080. (doi:10.1111/j.1558-5646.1995.tb04434.x)

14. Lynch M, Conery J, Bürger R. 1995 Mutation Accumulation and the Extinction of Small Populations. *Am. Nat.* **146**, 489–518.

15. Zeyl C, Mizesko M, De Visser JAGM. 2001 Mutational Meltdown in Laboratory Yeast Populations. *Evolution* **55**, 909–917. (doi:10.1111/j.0014-3820.2001.tb00608.x)

16. Shaw FH, Baer CF. 2011 Fitness-dependent mutation rates in finite populations. *J. Evol. Biol.* **24**, 1677–1684. (doi:10.1111/j.1420-9101.2011.02320.x)

17. Coron C, Méléard S, Porcher E, Robert A. 2013 Quantifying the Mutational Meltdown in Diploid Populations. *Am. Nat.* **181**, 623–636. (doi:10.1086/670022)

18. Lansch-Justen L, Cusseddu D, Schmitz MA, Bank C. 2022 The extinction time under mutational meltdown driven by high mutation rates. *Ecol. Evol.* **12**, e9046. (doi:10.1002/ece3.9046)

19. Olofsson P, Chipkin L, Daileda RC, Azevedo RBR. 2023 Mutational meltdown in asexual populations doomed to extinction. *J. Math. Biol.* **87**, 88. (doi:10.1007/s00285-023-02019-y)

20. Ruan Y, Wang H, Zhang L, Wen H, Wu C-I. 2020 Sex, fitness decline and recombination – Muller's ratchet vs. Ohta's ratchet. , 2020.08.06.240713. (doi:10.1101/2020.08.06.240713)

21. Kondrashov AS. 1995 Contamination of the genome by very slightly deleterious mutations: why have we not died 100 times over? *J. Theor. Biol.* **175**, 583–594. (doi:10.1006/jtbi.1995.0167)

22. Charlesworth B. 2013 Why We Are Not Dead One Hundred Times Over. *Evolution* **67**, 3354–3361. (doi:10.1111/evo.12195)

23. Schultz ST, Lynch M. 1997 Mutation and Extinction: The Role of Variable Mutational Effects, Synergistic Epistasis, Beneficial Mutations, and Degree of Outcrossing. *Evolution* **51**, 1363–1371. (doi:10.1111/j.1558-5646.1997.tb01459.x)

24. Whitlock MC. 2000 Fixation of New Alleles and the Extinction of Small Populations: Drift Load, Beneficial Alleles, and Sexual Selection. *Evolution* **54**, 1855–1861.

25. Poon A, Otto SP. 2000 Compensating for Our Load of Mutations: Freezing the Meltdown of Small Populations. *Evolution* **54**, 1467–1479. (doi:10.1111/j.0014-3820.2000.tb00693.x)

26. Matheson J, Hernández U, Bertram J, Masel J. 2025 Human deleterious mutation rate slows adaptation and implies high fitness variance. *bioRxiv* , 2023.09.01.555871. (doi:10.1101/2023.09.01.555871)

27. Rousselle M, Simion P, Tilak M-K, Figuet E, Nabholz B, Galtier N. 2020 Is adaptation limited by mutation? A timescale-dependent effect of genetic diversity on the adaptive substitution rate in animals. *PLOS Genet.* **16**, e1008668. (doi:10.1371/journal.pgen.1008668)

28. Osmond MM, Klausmeier CA. 2017 An evolutionary tipping point in a changing environment. *Evolution* **71**, 2930–2941. (doi:10.1111/evo.13374)

29. Melissa MJ, Desai MM. 2024 A dynamical limit to evolutionary adaptation. *Proc. Natl. Acad. Sci.* **121**, e2312845121. (doi:10.1073/pnas.2312845121)

30. Park S-C, Krug J. 2007 Clonal interference in large populations. *Proc. Natl. Acad. Sci.* **104**, 18135–18140. (doi:10.1073/pnas.0705778104)

31. Charlesworth B, Jensen JD. 2021 Effects of Selection at Linked Sites on Patterns of Genetic Variability. *Annu. Rev. Ecol. Evol. Syst.* **52**, 177–197. (doi:10.1146/annurev-ecolsys-010621-044528)

32. Keightley PD, Otto SP. 2006 Interference among deleterious mutations favours sex and recombination in finite populations. *Nature* **443**, 89–92. (doi:10.1038/nature05049)

33. Barton NH, Otto SP. 2005 Evolution of Recombination Due to Random Drift. *Genetics* **169**, 2353–2370. (doi:10.1534/genetics.104.032821)

34. Sohail M *et al.* 2017 Negative selection in humans and fruit flies involves synergistic epistasis. *Science* **356**, 539–542. (doi:10.1126/science.aah5238)

35. Lee YCG. 2022 Synergistic epistasis of the deleterious effects of transposable elements. *Genetics* **220**, iyab211. (doi:10.1093/genetics/iyab211)

36. Matheson J, Masel J. 2024 Background Selection From Unlinked Sites Causes Nonindependent Evolution of Deleterious Mutations. *Genome Biol. Evol.* **16**, evae050. (doi:10.1093/gbe/evae050)

37. Lesecque Y, Keightley PD, Eyre-Walker A. 2012 A Resolution of the Mutation Load Paradox in Humans. *Genetics* **191**, 1321–1330. (doi:10.1534/genetics.112.140343)

38. Eőry L, Halligan DL, Keightley PD. 2010 Distributions of Selectively Constrained Sites and Deleterious Mutation Rates in the Hominid and Murid Genomes. *Mol. Biol. Evol.* **27**, 177–192. (doi:10.1093/molbev/msp219)

39. Wang Y, Obbard DJ. 2023 Experimental estimates of germline mutation rate in eukaryotes: a phylogenetic meta-analysis. *Evol. Lett.* **7**, 216–226. (doi:10.1093/evlett/qrad027)

40. Reed DH. 2005 Relationship between population size and fitness. *Conserv. Biol.* **19**, 235.

41. Kondrashov AS. 2017 *Crumbling Genome: The Impact of Deleterious Mutations on Humans*. New Jersey, US: John Wiley & Sons.

42. Haller BC, Messer PW. 2019 SLiM 3: Forward Genetic Simulations Beyond the Wright–Fisher Model. *Mol. Biol. Evol.* **36**, 632–637. (doi:10.1093/molbev/msy228)

43. McCandlish DM, Epstein CL, Plotkin JB. 2015 Formal properties of the probability of fixation: Identities, inequalities and approximations. *Theor. Popul. Biol.* **99**, 98–113. (doi:10.1016/j.tpb.2014.11.004)

44. Ewens WJ. 2004 Discrete Stochastic Models. In *Mathematical Population Genetics 1: Theoretical Introduction*, pp. 104–109. Springer Science & Business Media.

45. Kim BY, Huber CD, Lohmueller KE. 2017 Inference of the Distribution of Selection Coefficients for New Nonsynonymous Mutations Using Large Samples. *Genetics* **206**, 345–361. (doi:10.1534/genetics.116.197145)

46. Kryukov GV, Schmidt S, Sunyaev S. 2005 Small fitness effect of mutations in highly conserved non-coding regions. *Genetics* **14**, 2221–2229.

47. Di C, Ramesh S, Ernst J, Lohmueller KE. 2025 The landscape of fitness effects of putatively functional noncoding mutations in humans. , 2025.05.14.654124. (doi:10.1101/2025.05.14.654124)

48. VanValen L. 1973 A New Evolutionary Law. *Evol. Theory* **1**, 1–30.

49. Bertram J, Masel J. 2019 Density-dependent selection and the limits of relative fitness. *Theor. Popul. Biol.* **129**, 81–92. (doi:10.1016/j.tpb.2018.11.006)

50. Draghi JA, McGlothlin JW, Kindsvater HK. 2024 Demographic feedbacks during evolutionary rescue can slow or speed adaptive evolution. *Proc. R. Soc. B Biol. Sci.* **291**, 20231553. (doi:10.1098/rspb.2023.1553)

51. Pardo-Manuel de Villena F, Sapienza C. 2001 Recombination is proportional to the number of chromosome arms in mammals. *Mamm. Genome* **12**, 318–322. (doi:10.1007/s003350020005)

52. Kelleher J, Thornton KR, Ashander J, Ralph PL. 2018 Efficient pedigree recording for fast population genetics simulation. *PLOS Comput. Biol.* **14**, e1006581. (doi:10.1371/journal.pcbi.1006581)

53. Charlesworth B. 1994 The effect of background selection against deleterious mutations on weakly selected, linked variants. *Genet. Res.* **63**, 213–227. (doi:10.1017/S0016672300032365)

54. Peck JR. 1994 A ruby in the rubbish: beneficial mutations, deleterious mutations and the evolution of sex. *Genetics* **137**, 597–606. (doi:10.1093/genetics/137.2.597)

55. Good BH, Desai MM. 2014 Deleterious Passengers in Adapting Populations. *Genetics* **198**, 1183–1208. (doi:10.1534/genetics.114.170233)

56. Pénisson S, Singh T, Sniegowski P, Gerrish P. 2017 Dynamics and Fate of Beneficial Mutations Under Lineage Contamination by Linked Deleterious Mutations. *Genetics* **205**, 1305–1318. (doi:10.1534/genetics.116.194597)

57. Galeota-Sprung B, Sniegowski P, Ewens W. 2020 Mutational Load and the Functional Fraction of the Human Genome. *Genome Biol. Evol.* **12**, 273–281. (doi:10.1093/gbe/evaa040)

58. Gomulkiewicz R, Holt RD. 1995 When does Evolution by Natural Selection Prevent Extinction? *Evolution* **49**, 201–207. (doi:10.2307/2410305)

59. Gonzalez A, Ronce O, Ferriere R, Hochberg ME. 2013 Evolutionary rescue: an emerging focus at the intersection between ecology and evolution. *Philos. Trans. R. Soc. B Biol. Sci.* **368**, 20120404. (doi:10.1098/rstb.2012.0404)

60. Alexander HK, Martin G, Martin OY, Bonhoeffer S. 2014 Evolutionary rescue: linking theory for conservation and medicine. *Evol. Appl.* **7**, 1161–1179. (doi:10.1111/eva.12221)

61. Carlson SM, Cunningham CJ, Westley PAH. 2014 Evolutionary rescue in a changing world. *Trends Ecol. Evol.* **29**, 521–530. (doi:10.1016/j.tree.2014.06.005)

534 62. Bell G. 2017 Evolutionary Rescue. *Annu. Rev. Ecol. Evol. Syst.* **48**, 605–627.
535 (doi:10.1146/annurev-ecolsys-110316-023011)

536 63. Orr HA, Unckless RL. 2008 Population Extinction and the Genetics of Adaptation. *Am. Nat.* **172**,
537 160–169. (doi:10.1086/589460)

538 64. Martin G, Aguilée R, Ramsayer J, Kaltz O, Ronce O. 2013 The probability of evolutionary rescue:
539 towards a quantitative comparison between theory and evolution experiments. *Philos. Trans. R.*
540 *Soc. B Biol. Sci.* **368**, 20120088. (doi:10.1098/rstb.2012.0088)

541 65. Orr HA, Unckless RL. 2014 The Population Genetics of Evolutionary Rescue. *PLoS Genet.* **10**,
542 e1004551. (doi:10.1371/journal.pgen.1004551)

543 66. Uecker H, Otto SP, Hermisson J. 2014 Evolutionary Rescue in Structured Populations. *Am. Nat.*
544 **183**, E17–E35. (doi:10.1086/673914)

545 67. Uecker H, Hermisson J. 2016 The Role of Recombination in Evolutionary Rescue. *Genetics* **202**,
546 721–732. (doi:10.1534/genetics.115.180299)

547 68. Wilson BA, Pennings PS, Petrov DA. 2017 Soft Selective Sweeps in Evolutionary Rescue.
548 *Genetics* **205**, 1573–1586. (doi:10.1534/genetics.116.191478)

549 69. Shaffer ML. 1981 Minimum Population Sizes for Species Conservation. *BioScience* **31**, 131–134.
550 (doi:10.2307/1308256)

551 70. Lacava J, Hughes J. 1984 Determining Minimum Viable Population Levels. *Wildl. Soc. Bull. 1973-*
552 *2006* **12**, 370–376.

553 71. Reed DH, O'Grady JJ, Brook BW, Ballou JD, Frankham R. 2003 Estimates of minimum viable
554 population sizes for vertebrates and factors influencing those estimates. *Biol. Conserv.* **113**, 23–34.
555 (doi:10.1016/S0006-3207(02)00346-4)

556 72. Traill LW, Bradshaw CJA, Brook BW. 2007 Minimum viable population size: A meta-analysis of
557 30 years of published estimates. *Biol. Conserv.* **139**, 159–166. (doi:10.1016/j.biocon.2007.06.011)

558 73. Nabutanyi P, Wittmann MJ. 2022 Modeling minimum viable population size with multiple genetic
559 problems of small populations. *Conserv. Biol.* **36**, e13940. (doi:10.1111/cobi.13940)

560 74. Nunney L, Campbell KA. 1993 Assessing minimum viable population size: Demography meets
561 population genetics. *Trends Ecol. Evol.* **8**, 234–239. (doi:10.1016/0169-5347(93)90197-W)

562 75. Johri P, Charlesworth B, Jensen JD. 2020 Toward an Evolutionarily Appropriate Null Model:
563 Jointly Inferring Demography and Purifying Selection. *Genetics* **215**, 173–192.
564 (doi:10.1534/genetics.119.303002)

565 76. Murphy DA, Elyashiv E, Amster G, Sella G. 2022 Broad-scale variation in human genetic diversity
566 levels is predicted by purifying selection on coding and non-coding elements. *eLife* **12**, e76065.
567 (doi:10.7554/eLife.76065)

568 77. Buffalo V, Kern AD. 2024 A quantitative genetic model of background selection in humans. *PLOS*
569 *Genet.* **20**, e1011144. (doi:10.1371/journal.pgen.1011144)

570 78. Charlesworth B. 2013 Background Selection 20 Years on: The Wilhelmine E. Key 2012
571 Invitational Lecture. *J. Hered.* **104**, 161–171. (doi:10.1093/jhered/ess136)

572 79. IUCN. 2025 The IUCN Red List of Threatened Species. *IUCN Red List Threat. Species*. See
573 https://www.iucnredlist.org (accessed on 3 October 2025).

574 80. Pacifici M *et al.* 2015 Assessing species vulnerability to climate change. *Nat. Clim. Change* **5**,
575 215–224. (doi:10.1038/nclimate2448)

576 81. Santidrián Tomillo P, Wallace BP, Paladino FV, Spotila JR, Genovart M. 2021 Short-term gain,
577 long-term loss: How a widely-used conservation tool could further threaten sea turtles. *Biol.*
578 *Conserv.* **261**, 109260. (doi:10.1016/j.biocon.2021.109260)

579 82. Rout TM, Hauser CE, Possingham HP. 2007 Minimise long-term loss or maximise short-term
580 gain?: Optimal translocation strategies for threatened species. *Ecol. Model.* **201**, 67–74.
581 (doi:10.1016/j.ecolmodel.2006.07.022)

582 83. Bottrill MC *et al.* 2008 Is conservation triage just smart decision making? *Trends Ecol. Evol.* **23**,
583 649–654. (doi:10.1016/j.tree.2008.07.007)

584 84. Vucetich JA, Nelson MP, Bruskotter JT. 2017 Conservation Triage Falls Short Because
585 Conservation Is Not Like Emergency Medicine. *Front. Ecol. Evol.* **5**.
586 (doi:10.3389/fevo.2017.00045)

587 85. Willis KJ, Birks HJB. 2006 What Is Natural? The Need for a Long-Term Perspective in
588 Biodiversity Conservation. *Science* **314**, 1261–1265. (doi:10.1126/science.1122667)

589 86. Barnosky AD *et al.* 2017 Merging paleobiology with conservation biology to guide the future of
590 terrestrial ecosystems. *Science* **355**, eaah4787. (doi:10.1126/science.aah4787)

591 87. Whiteley AR, Fitzpatrick SW, Funk WC, Tallmon DA. 2015 Genetic rescue to the rescue. *Trends*
592 *Ecol. Evol.* **30**, 42–49. (doi:10.1016/j.tree.2014.10.009)

593 88. Frankham R, Ballou JD, Ralls K, Eldridge M, Dudash MR, Fenster CB, Lacy RC, Sunnucks P.
594 2017 *Genetic Management of Fragmented Animal and Plant Populations*. Oxford U.K.: Oxford
595 University Press.

596 89. Bell DA, Robinson ZL, Funk WC, Fitzpatrick SW, Allendorf FW, Tallmon DA, Whiteley AR.
597 2019 The Exciting Potential and Remaining Uncertainties of Genetic Rescue. *Trends Ecol. Evol.*
598 **34**, 1070–1079. (doi:10.1016/j.tree.2019.06.006)

599 90. Ralls K, Ballou JD, Dudash MR, Eldridge MDB, Fenster CB, Lacy RC, Sunnucks P, Frankham R.
600 2018 Call for a Paradigm Shift in the Genetic Management of Fragmented Populations. *Conserv.*
601 *Lett.* **11**, e12412. (doi:10.1111/conl.12412)

602 91. Ralls K, Sunnucks P, Lacy RC, Frankham R. 2020 Genetic rescue: A critique of the evidence
603 supports maximizing genetic diversity rather than minimizing the introduction of putatively
604 harmful genetic variation. *Biol. Conserv.* **251**, 108784. (doi:10.1016/j.biocon.2020.108784)

605 92. Bijlsma R, Westerhof MDD, Roekx LP, Pen I. 2010 Dynamics of genetic rescue in inbred
606 Drosophila melanogaster populations. *Conserv. Genet.* **11**, 449–462. (doi:10.1007/s10592-010-
607 0058-z)

608 93. Pérez-Pereira N, Caballero A, García-Dorado A. 2022 Reviewing the consequences of genetic
609 purging on the success of rescue programs. *Conserv. Genet.* **23**, 1–17. (doi:10.1007/s10592-021-
610 01405-7)

611 94. Chen N, Cosgrove EJ, Bowman R, Fitzpatrick JW, Clark AG. 2016 Genomic Consequences of
612 Population Decline in the Endangered Florida Scrub-Jay. *Curr. Biol.* **26**, 2974–2979.
613 (doi:10.1016/j.cub.2016.08.062)

614 95. 2025 MaselLab/MutationLoad: C1.0.0. (doi:10.5281/zenodo.17281300)

615